

ZnO epilayers on GaN templates: Polarity control and valence-band offset

Soon-Ku Hong,^{a)} Takashi Hanada, Hisao Makino, Hang-Ju Ko, Yefan Chen,
and Takafumi Yao

Institute for Materials Research, Tohoku University, 2-1-1 Katahira, Aoba-ku, Sendai 980-8577, Japan

Akinori Tanaka, Hiroyuki Sasaki, and Shigeru Sato

Department of Physics, Tohoku University, Sendai 980-8578, Japan

Daisuke Imai, Kiyooki Araki, and Makoto Shinohara

Surface Analysis and Semiconductor Equipment Division, Shimadzu Corporation, 380-1 Horiyamashita, Hadano-shi, Kanagawa 259-1304, Japan

(Received 28 December 2000; accepted 5 March 2001)

We report on the growth of polarity-controlled ZnO epilayers by plasma-assisted molecular-beam epitaxy and the measurement of valence-band offset at the ZnO/GaN heterointerface. The polarity of ZnO epilayers is determined by coaxial-impact-collision ion-scattering spectroscopy. The band offset is determined by ultraviolet and x-ray photoelectron spectroscopy. The high-resolution transmission electron microscopy study reveals the formation of an interface layer between the ZnO and GaN epilayers in O-plasma preexposed samples, while no interface layer is formed in Zn preexposed samples. Zn preexposure prior to ZnO growth results in Zn-polar ZnO epilayers (Zn face), while O-plasma preexposure leads to the growth of O-polar ZnO epilayers (O face). The interface layer is identified to be single-crystalline, monoclinic Ga₂O₃. The estimated valence band offset at the ZnO/GaN(0001) heterojunction with Zn preexposure is 0.8 eV with a type-II band alignment. © 2001 American Vacuum Society. [DOI: 10.1116/1.1374630]

I. INTRODUCTION

GaN, ZnO, and related alloys are wurtzite-structure wide-band-gap semiconductors and have attracted considerable attention because of their applications to short-wavelength light-emitting devices. Those materials have been grown with the *c* axis parallel to the growth direction, which results in either cation-polar or anion-polar layers. It has been demonstrated that the lattice polarity has strong effects on growth, material property, and device performance.¹

Epitaxial layers with opposite polarity can be easily obtained by changing the polarity of the substrate, if polar substrates with both polarities are available. There have been only few reports on the control of the lattice polarity of epilayers grown on nonpolar substrates. The growth of GaN epilayers with different lattice polarities on nonpolar Al₂O₃ substrates has been achieved by employing different initial processes, including surface nitridation, buffer-layer growth, and annealing. In the case of ZnO epilayers on nonpolar Al₂O₃ substrates, only O-polar ZnO growth has been reported.²

This article will report the plasma-assisted molecular-beam epitaxy (PMBE) growth of polarity-controlled ZnO epilayers on Ga-polar (0001) GaN templates by engineering the ZnO/GaN heterointerface, and band alignment at a ZnO/GaN heterointerface, determined by ultraviolet and x-ray photoelectron spectroscopies (UPS and XPS). We note here that there have been no experimental studies on the band offset at a ZnO/GaN heterointerface.

II. GROWTH OF POLARITY-CONTROLLED ZnO EPILAYERS ON GaN TEMPLATES

The substrates used in this study are Ga-polar (0001) GaN epilayers (4 μm-thick), grown on *c*-Al₂O₃ by metal-organic chemical-vapor deposition (MOCVD). ZnO epilayers were grown on the GaN templates by PMBE using a radio-frequency oxygen-plasma source and a Zn solid source. Detailed procedures for substrate cleaning and PMBE growth conditions have been reported elsewhere.³ Zn- or O-plasma preexposure after thermal cleaning of GaN surfaces was carried out at 700 °C for 3 min prior to ZnO growth. ZnO epilayers were grown at the same temperature.

Figure 1 shows high-resolution transmission electron microscopy (HRTEM) micrographs of the ZnO/GaN interfaces for (a) Zn- and (b) O-plasma preexposures. The remarkable difference in these two types of interface is the formation of an interface layer in the case of O-plasma preexposure, while no interface layer is formed by Zn preexposure. The thickness of the interface layer at the ZnO/GaN interface with O-plasma preexposure is estimated to be about 3.5 nm regardless of O-plasma preexposure time for 1–15 min. The interface layer is identified as single-crystalline monoclinic Ga₂O₃ by diffraction pattern analysis in which the (001) plane of Ga₂O₃ is parallel to the (0001) plane of GaN or ZnO.

The epitaxy relationship between ZnO and GaN with the Ga₂O₃ interface layer was found to be

$$[2-1-10]_{\text{ZnO}} \parallel [010]_{\text{Ga}_2\text{O}_3} \parallel [2-1-10]_{\text{GaN}}$$

and

$$(0001)_{\text{ZnO}} \parallel (001)_{\text{Ga}_2\text{O}_3} \parallel (0001)_{\text{GaN}}.$$

^{a)}Author to whom correspondence should be addressed; electronic mail: skhong@imr.tohoku.ac.jp

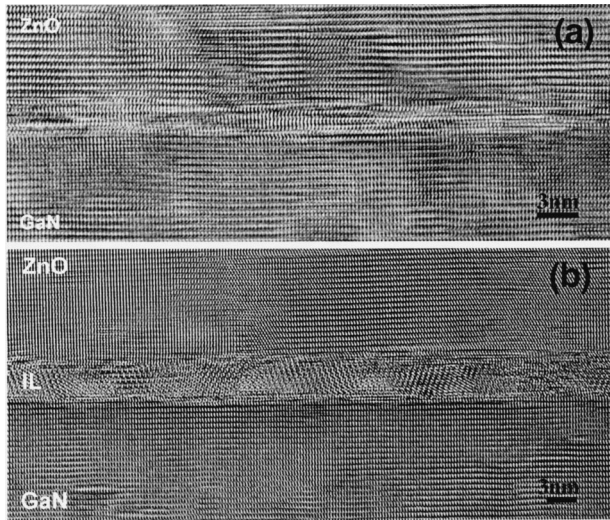


FIG. 1. HRTEM micrographs for (a) Zn preexposed and (b) O-plasma preexposed samples viewed along the $[2\text{-}1\text{-}10]$ direction. There is no interface layer between the ZnO/GaN heterointerface for the Zn preexposed sample (a), while a 3.5-nm-thick interface layer is formed between the ZnO/GaN heterointerface for the O-plasma preexposed ZnO sample (b). The interface layer is identified as monoclinic Ga_2O_3 . Details are described in the text.

This epitaxial relationship would give rise to lattice strain in the Ga_2O_3 interface layer due to lattice misfit with the GaN substrate or with the ZnO overlayer. Although the lattice constant of Ga_2O_3 along the $[010]$ direction (0.304 nm) is slightly smaller than the corresponding lattice parameters of GaN (0.319 nm) and ZnO (0.325 nm) along the $[2\text{-}1\text{-}10]$ direction, the lattice constant of Ga_2O_3 along a $[100]$ direction (1.223 nm) is about four times larger than those of GaN and ZnO along the $[01\text{-}10]$ direction. Therefore, we have adapted the concept of domain matching epitaxy;⁴ matching of one unit of Ga_2O_3 along $[100]$ with four units of GaN or ZnO along $[01\text{-}10]$. Accordingly, the lattice misfits along the $[010]$ ($b=0.304$ nm) and the $[100]$ ($a=1.223$ nm) axes of Ga_2O_3 with the corresponding GaN $[2\text{-}1\text{-}10]$ ($a=0.319$ nm) and $[01\text{-}10]$ ($4\sqrt{3}a/2=1.105$ nm) directions are reduced to -4.7% and 10.7% , respectively. The lattice misfits of Ga_2O_3 and ZnO along the corresponding directions are also reduced to -6.5% and 8.6% , respectively.

The different interface structures for Zn- and O-plasma preexposures offer a possibility of controlling the lattice polarity of ZnO epilayers. On exposing Zn beams onto a Ga-polar (0001) GaN surface, Ga–Zn bonds may be initially formed at the surface. It is likely, however, that the Zn atoms will be replaced with O atoms to form stronger Ga–O–Zn bonding during ZnO growth, since the Zn–Ga (cation–cation) bonding is weak and unstable⁵ compared with Ga–O and Zn–O (cation–anion) bondings. The bond energies of Ga–O and Zn–O are 353.6 and 270.7 kJ/mol, respectively.⁶ Although no data are available for Zn–Ga bonding, it is most likely that the bonding energy of Zn–Ga is much weaker than Ga–O and Zn–O because of weaker metallic bonding. Therefore, a “N–Ga–O–Zn” stacking sequence at the interface can be expected in the Zn preexposed samples, which should result in a Zn-polar (0001) ZnO epilayer.

In the case of O-plasma preexposure, the existence of a Ga_2O_3 interface layer affects bonding sequence at the interface. The atomic plane in a Ga_2O_3 unit cell parallel to the interface is either the O or Ga plane. It is most likely that an O plane is formed in the Ga_2O_3 layer at the $\text{Ga}_2\text{O}_3/\text{GaN}$ interface to form O–Ga bonding with the topmost Ga atoms at the GaN template surface. If this is the case, the Ga_2O_3 interface layer must have an O-terminated top surface, since half of the unit cell parallel to the interface also has an O-terminated surface and half of the unit cell satisfies the ratio of Ga/O as $2/3$ as well as a unit cell, which satisfies the stoichiometry of Ga_2O_3 . Other terminations do not satisfy the $2/3$ ratio of the Ga/O, which implies that the O termination at half of the unit cell or one unit cell parallel to the interface is stable. Here, it should be noted that the HRTEM micrograph [Fig. 1(b)] of the Ga_2O_3 interface layer shows well-defined planes parallel to the interface with the inter-plane distance corresponding to one or half of the Ga_2O_3 unit cell. Therefore, it is most likely that the O plane is formed to form O–Ga bondings at the $\text{Ga}_2\text{O}_3/\text{GaN}$ interface. The exposure of the Zn and O flux for ZnO growth followed by the O-plasma preexposure will lead to strong and stable Zn–O bondings at the ZnO/ Ga_2O_3 interface. The resultant stacking sequence at the interface in the O-plasma preexposed samples is a “N–Ga–(Ga_2O_3 Interface layer)–Zn–O,” which implies the growth of an O-polar (000-1) ZnO epilayer.

III. POLARITY OF Zn- AND O-PLASMA PREEXPOSED ZnO EPILAYERS

The lattice polarity of the ZnO epilayers was determined by coaxial-impact-collision ion-scattering spectroscopy (CAICISS) (Shimadzu Co., TALIS 9700). Primary He^+ ions with energy of 2 keV were used for the measurements. The polar angle dependence of CAICISS signals along the azimuth direction of $[11\text{-}20]$ was measured. Figure 2 shows experimental data (closed squares) and simulated (open circles) polar angle dependence of Zn signals from (a) Zn- and (b) O-plasma preexposed ZnO epilayers (here, the spectra are plotted as a function of incidence angle, which is equal to 90° minus the polar angle). The spectra for the two samples are significantly different. In the case of Zn preexposed ZnO epilayers, the observed angle dependence is characterized by three dominant peaks at $\theta=24^\circ$, 50° , and 74° . This feature agrees well with the simulated spectrum obtained for the Zn-polar ZnO. In the case of O-plasma preexposed ZnO epilayers, the experimental angle dependence is characterized by four dominant peaks at $\theta=22^\circ$, 36° , 54° , and a broad peak ranging from 72° to 76° . This feature also agrees well with the simulated spectrum obtained for the O-polar ZnO. The simulation algorithm used was based on the three-dimensional two-atom triple-scattering model.⁷ It should be noted that the present results agreed well with the reported CAICISS spectra from the Zn- and O faces of bulk ZnO.² Therefore, we conclude that Zn preexposed ZnO epilayers have a characteristic of Zn polarity, while O-plasma preexposed ZnO epilayers have a characteristic of O polarity.

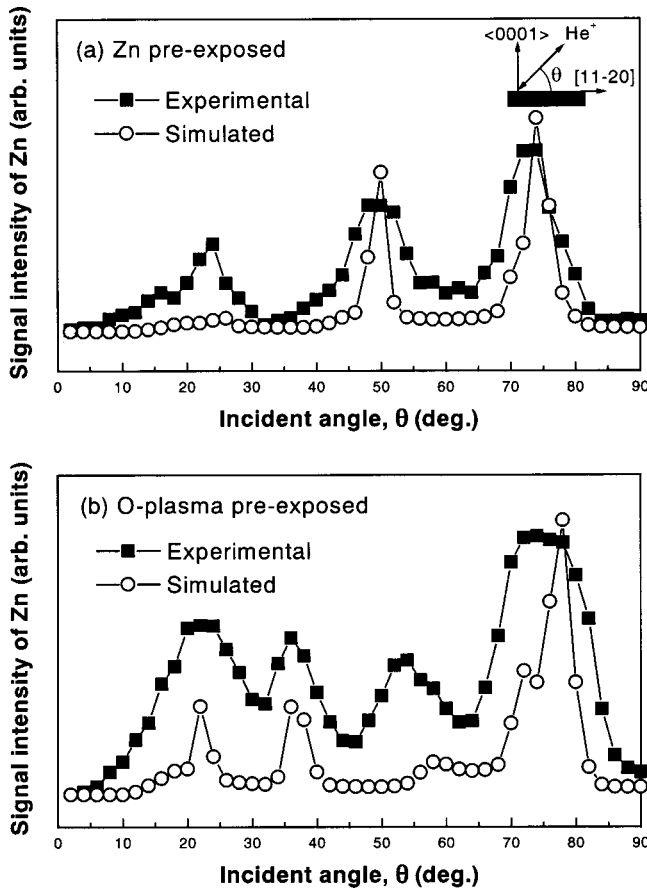


FIG. 2. Incidence-angle ($\theta=90^\circ$, polar angle) dependence of the Zn signal measured by CAICISS from the (a) Zn preexposed and (b) O-plasma preexposed ZnO epilayers. The setup for the measurements is the same for both experiments and are shown in (a).

The CAICISS results clearly indicate that we have selectively grown ZnO epilayers with both polarities by PMBE even on Ga-polar GaN. We stress that the observed polarity of the ZnO epilayers is the direct consequence of the interface bonding discussed in Sec. II.

The origin of such different characteristics of the CAICISS spectra can be understood by considering the surface structures of Zn- and O-polar ZnO, shadow cones formed by the surface Zn and O atoms, focusing, and shadowing effects of scattered ions. For example, in the case of a Zn-polar surface with an ion-incident angle of 36° , Zn atoms on the third and fifth layers are shadowed by O atoms on the second and fourth layers, respectively. Therefore, signals scattered from the Zn atoms are not observed. On the other hand, in the case of an O-polar surface with an ion-incident angle of 36° , Zn atoms on the second and fourth layers are not shadowed by O atoms on the first and third layers. Additionally, the focusing effect would occur because the Zn atoms on the fourth layer are located on the edge of shadow cones formed by the O atoms on the first layer, which results in strong signals scattered from the Zn atoms. The CAICISS spectra at other incident angles can be understood similarly.

IV. VALENCE BAND OFFSET AT THE ZnO/GaN HETEROINTERFACE

As shown in Fig. 1(b), an O-plasma preexposed ZnO epilayer on a GaN template has an interface layer between the ZnO and GaN epilayers. Hence, measurement of the band offset has been carried out for a Zn preexposed sample, which has no interface layer. Here, we used an *n*-type, MOCVD grown (0001) Ga-polar GaN epilayer on Al_2O_3 with a carrier concentration of $8.18 \times 10^{18} \text{ cm}^{-3}$ and a mobility of $197 \text{ cm}^2/\text{V s}$. The ZnO epilayers showed *n*-type conductivity.⁸

The method used to measure the valence-band discontinuity at the ZnO/GaN interface is similar to that of Waldrop and Grant.⁹ The basic scheme of this approach is to measure the valence-band maximum (VBM) energy relative to the core-level energy for each semiconductor and then use the measured difference between the two core-level energies at a junction between the two semiconductors to determine the discontinuity of the VBM. Based on this approach, the valence-band offset (ΔE_V) can be described by the following formula:

$$\Delta E_V(\text{ZnO/GaN}) = (3d - \text{VBM})_{\text{bulk}}^{\text{GaN}} - (3d - \text{VBM})_{\text{bulk}}^{\text{ZnO}} - (3d^{\text{GaN}} - 3d^{\text{ZnO}})_{\text{interface}}. \quad (1)$$

This method has been successfully applied for the evaluation of band offsets for various heterojunctions including AlN/GaN, GaAs/ZnSe, InN/GaN, and InN/AlN.^{9–12}

In order to estimate the valence-band offset, we have examined three kinds of samples: (1) A 4- μm -thick Ga-face GaN epilayer on sapphire grown by MOCVD, which was used as a substrate for the ZnO epilayer, for the determination of the VBM and Ga $3d$ energies of GaN. (2) A 65-nm-thick ZnO epilayer grown by PMBE for determination of the VBM and Zn $3d$ energies of ZnO. (3) A 2-nm-thick ZnO epilayer for determination of the difference between the Ga $3d$ and Zn $3d$ core-level energies at the ZnO/GaN heterointerface.

All UPS and XPS measurements were performed *ex situ* using an ultrahigh-vacuum (middle 10^{-11} Torr) XPS/UPS combined system. We have used ARUPS 10 (VG Co., Ltd.), equipped with a He I source (21.22 eV) with an energy resolution of 61.5 meV for the UPS measurements, and CLAM2 (VG Co., Ltd.), equipped with x-ray sources of Al $K\alpha$ (1486.5 eV) and Mg $K\alpha$ (1253.6 eV) for the XPS measurements. The measured binding energies are calibrated by using the Au $4f_{7/2}$ level (for XPS) and the Fermi edge of Au (for UPS). The UPS and XPS measurements were carried out after Ar^+ ion sputtering at an ion-beam voltage of 1.0–1.5 kV and current of 30–40 μA for 10–120 s in order to remove surface contaminations. The cleanness after Ar^+ -ion sputtering is checked by monitoring the intensities and positions of C $1s$ and O $1s$ peaks. All measurements were carried out at 40.2 K.

The difference in the VBM and the Ga $3d$ energies is determined to be 17.5 eV, which agrees well with previously

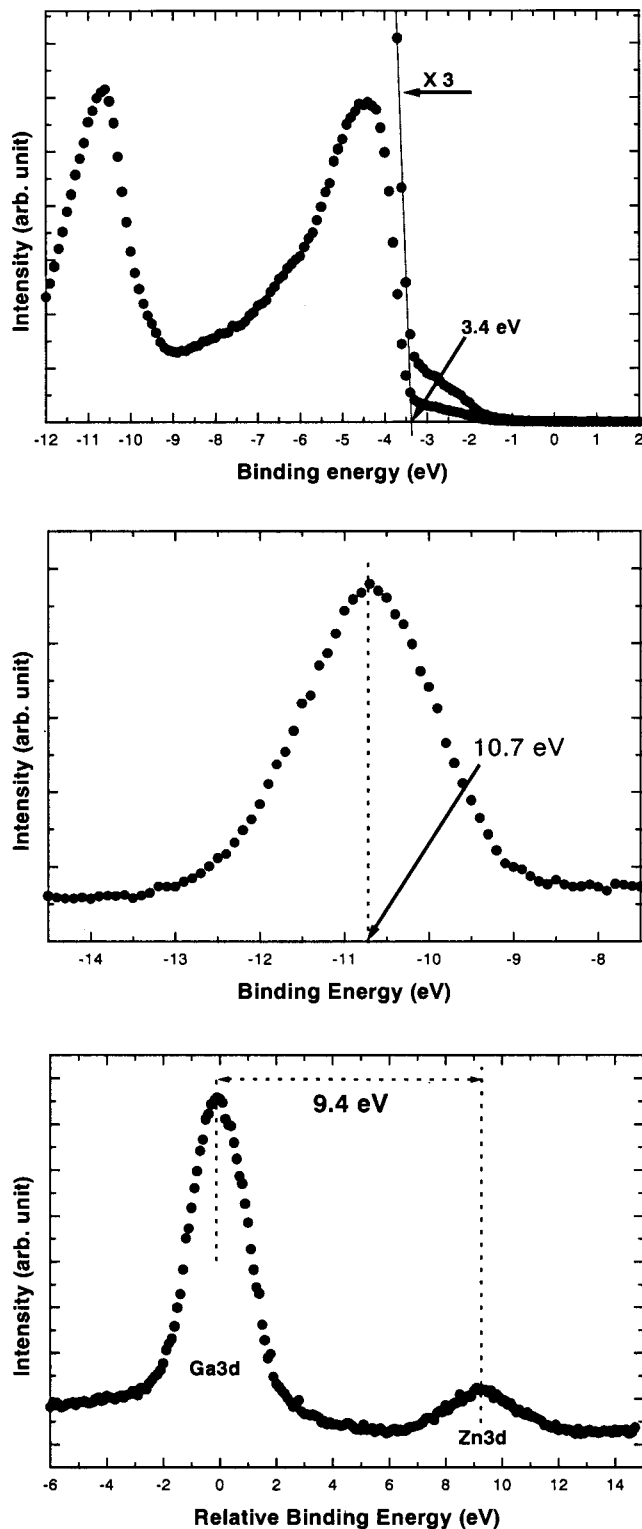


FIG. 3. (a) UPS VB spectrum from the 65-nm-thick ZnO epilayer. (b) XPS Zn 3d core-level spectrum from the 65-nm-thick ZnO epilayer. (c) XPS spectra (the Ga 3d level was set to be the origin of the energy axis) of Ga 3d and Zn 3d core levels from a 2-nm-thick ZnO epilayer grown on a 4- μ m-thick GaN epilayer.

reported values of 17.1–18.4 eV.¹² The VBM of GaN was determined to be 1.9 eV from UPS measurements, which agrees well with the reported value.¹³ The binding energy of the Ga 3d core level was determined to be 19.4 eV by XPS

measurements, which also agrees well with the reported value.¹³

Figure 3(a) shows an UPS VB spectrum of a 65-nm-thick ZnO epilayer. The features of the VB spectrum agree very well with the previously reported UPS spectrum of (0001) ZnO.¹⁴ From Fig. 3(a), we have determined the VBM energy to be 3.4 eV, which agrees well with the reported value.¹⁴ The core-level energy of Zn 3d determined by the XPS measurement is 10.7 eV, as shown in Fig. 3(b), which also agrees well with the reported values.^{14,15} Therefore, the difference in the VBM and the Zn 3d energies is determined to be 7.3 eV.

Figure 3(c) shows the relative energy positions (the center of the Ga 3d peak is set as zero) of the Ga 3d and Zn 3d core-level peaks obtained from a 2-nm-thick ZnO sample. The difference between the core-level energies between Ga 3d and Zn 3d is determined to be 9.4 eV. Based on the XPS and UPS data from the thick ZnO and thick GaN epilayers and the ZnO/GaN interface, we have determined the valence-band offsets at the ZnO/GaN heterointerface to be 0.8 eV with a type-II band alignment. Figure 4 shows a schematic flatband diagram for the (0001) ZnO/GaN heterojunction determined in the present study. We note that the theoretical valence-band offset for ZnO/GaN heterointerfaces is 1.0–2.2 eV.¹⁶

V. CONCLUSIONS

We have selectively grown both Zn- and O-polar ZnO epilayers by PMBE on Ga-polar GaN templates and experimentally determined the valence-band offset at the (0001) ZnO/GaN heterointerface. Zn preexposure prior to ZnO growth leads to the growth of Zn-polar ZnO epilayers, while O-plasma preexposure prior to ZnO growth results in the growth of O-polar epilayers. An interface layer was formed between the ZnO and GaN epilayers in the O-plasma preexposed sample and it is identified as single-crystalline, monoclinic Ga₂O₃. No interface layer is formed in the Zn preexposed sample. The origin of the different lattice polarities of the ZnO epilayers on Ga-polar GaN can be explained successfully by the proposed bonding sequences at the hetero-

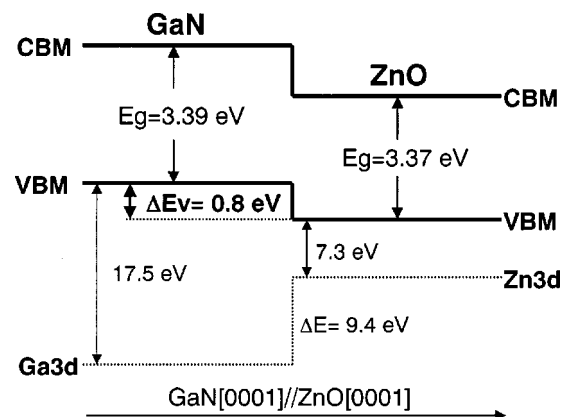


FIG. 4. Schematic band diagram for the ZnO/GaN heterointerface with Zn preexposure determined by UPS and XPS measurements.

interfaces for the two types of samples based on bonding stability and HRTEM observations. From UPS and XPS measurements, the valence-band offset at the (0001) ZnO/GaN heterointerface without the interface layer is determined to be 0.8 eV with a type-II band alignment.

ACKNOWLEDGMENT

One of the authors (S.-K.H.) would like to thank the International Communications Foundation (ICF) for its financial support under the "Fellowship for Researchers and Graduate Students from Abroad."

¹E. S. Hellman, MRS Internet J. Nitride Semicond. Res. **3**, 11 (1998).

²T. Ohnishi, A. Ohtomo, M. Kawasaki, K. Takahashi, M. Yoshimoto, and H. Koinuma, Appl. Phys. Lett. **72**, 824 (1998).

³S. K. Hong, H. J. Ko, Y. Chen, T. Hanada, and T. Yao, Appl. Surf. Sci. **159-160**, 441 (2000).

⁴T. Zheleva, K. Jagannadham, and J. Narayan, J. Appl. Phys. **75**, 860 (1994).

⁵J. C. Philips, *Bonds and Bands in Semiconductors* (Academic, New York, 1973).

⁶*Handbook of Chemistry and Physics*, 70th ed. (CRC, Cleveland, OH, 1989).

⁷M. Shinohara, O. Ishiyama, F. Ohtani, M. Yoshimoto, T. Maeda, and H. Koinuma, *Proceedings of the 2nd NIRIM International Symposium on Advanced Materials*, Tsukuba, Japan (1995), p. 203; S. Sonoda, S. Shimizu, Y. Suzuki, K. Balakrishnan, J. Shirakashi, H. Okumura, T. Nishihara, and M. Shinohara, Jpn. J. Appl. Phys., Part 2 **38**, L1219 (1999).

⁸Y. Chen, S. K. Hong, H. J. Ko, M. Nakajima, T. Yao, and Y. Segawa, Appl. Phys. Lett. **76**, 245 (2000).

⁹J. R. Waldrop and R. W. Grant, Appl. Phys. Lett. **68**, 2879 (1996).

¹⁰M. Funato, S. Aoki, S. Fujita, and S. Fujita, J. Appl. Phys. **85**, 1514 (1999).

¹¹G. Martin, A. Botchkarey, A. Rockett, and H. Morkoc, Appl. Phys. Lett. **68**, 2541 (1996).

¹²S. W. King, C. Ronning, R. F. Davis, M. C. Benjamin, and R. J. Nemanich, J. Appl. Phys. **84**, 2086 (1998).

¹³J. Ma, B. Garni, N. Perkins, W. L. O'Brien, T. F. Kuech, and M. G. Lagally, Appl. Phys. Lett. **69**, 3351 (1996).

¹⁴R. T. Girard, O. Tjernberg, G. Chiaia, S. Soderholm, U. O. Karlsson, C. Wigren, H. Nysten, and I. Lindau, Surf. Sci. **373**, 409 (1997).

¹⁵L. Ley, R. A. Pollak, F. R. McFeely, S. P. Kowalczyk, and D. A. Shirley, Phys. Rev. B **9**, 600 (1974).

¹⁶T. Nakayama and M. Murayama, J. Cryst. Growth **214/215**, 299 (2000).